Inorg. Chem. **2006**, *45*, 162–173

Inorganic Chemistry
Article

Syntheses, Crystal Structures, and Magneto–Structural Correlations of Novel Cu^{II} Complexes Containing a Planar $[\mathrm{Cu}(\mu\text{-}\mathrm{L}^1)]_2$ (HL^1 = 3-(2-Pyridyl)pyrazole) Unit: From Dinuclear to Tetranuclear and Then to One-Dimensional Compounds

Tong-Liang Hu,[†] Jian-Rong Li,[†] Chun-Sen Liu,[†] Xue-Song Shi,[†] Jiang-Ning Zhou,[†] Xian-He Bu,*,[†] and Joan Ribas[‡]

Department of Chemistry, Nankai University, Tianjin 300071, P. R. China, and Departament de Química Inorgànica, Universitat de Barcelona, Diagonal 647, 08028 Barcelona, Spain

Received August 31, 2005

Seven new Cu^{II} complexes based on a binuclear planar unit $[\mathrm{Cu}(\mu\text{-}\mathbf{L}^1)]_2$, $\{[\mathrm{Cu}(\mu\text{-}\mathbf{L}^1)(\mathrm{NO_3})(\mathrm{H_2O})]_2$ (**1**), $[\mathrm{Cu}(\mu\text{-}\mathbf{L}^1)(\mathrm{H}\mathbf{L}^1)(\mathrm{ClO_4})]_2$ (**2**), $[\mathrm{Cu_4}(\mu\text{-}\mathbf{L}^1)_6(\mathrm{NO_3})_2]$ (**3**), $[\mathrm{Cu_4}(\mu\text{-}\mathbf{L}^1)_6(\mathbf{L}^1)_2]$ (**4**), $[\mathrm{Cu_4}(\mu\text{-}\mathbf{L}^1)_6(\mu\text{-}\mathbf{L}^2)]_n$ (**5**), $[\mathrm{Cu_4}(\mu\text{-}\mathbf{L}^1)_6(\mu\text{-}\mathbf{L}^3)]_n$ (**6**), $\{[\mathrm{Cu_4}(\mu\text{-}\mathbf{L}^1)_4(\mu\text{-}\mathbf{L}^4)_2](\mathrm{H_2O})_3\}_n$ (**7**) ($\mathrm{H}\mathbf{L}^1$ = 3-(2-pyridyl)pyrazole, $\mathbf{L}^2$ = 1,8-naphthalenedicarboxylate, $\mathbf{L}^3$ = terephthalate, $\mathbf{L}^4$ = 2,6-pyridinedicarboxylate)}, have been synthesized and characterized by elemental analysis, IR, and X-ray diffraction. In **1** and **2**, the Cu^{II} centers are linked by deprotonated pyrazolyl groups to form dinuclear structures. **3** and **4** have similar gridlike tetranuclear structures in which two additional deprotonated $\mathbf{L}^1$ ligands bridge two $[\mathrm{Cu}(\mu\text{-}\mathbf{L}^1)]_2$ units perpendicularly. **5** and **6** consist of similar one-dimensional (1-D) chains in which gridlike tetranuclear copper(II) units similar to that of **3** are further linked by $\mathbf{L}^2$ or $\mathbf{L}^3$ ligands, respectively. And, in **7**, $\mathbf{L}^4$ ligands link $[\mathrm{Cu}(\mu\text{-}\mathbf{L}^1)]_2$ binuclear units to form a tetranuclear gridlike structure in chelating/bridging mode and simultaneously bridge the tetranuclear units to form a 1-D chain. The magnetic properties of all complexes were studied by variable-temperature magnetic susceptibility and magnetization measurements. The obtained parameters of J range from -33.1 to -211 cm^{-1}, indicating very strong antiferromagnetic coupling between Cu^{II} ions. The main factor that affects the $|J|$ parameter is the geometry of the $\mathrm{Cu(N_2)_2Cu}$ entity. From the magnetic point of view, **1** and **2** feature “pure” dinuclear, **3** and **5** tetranuclear, and **4**, **6**, and **7** pseudodinuclear moieties.

Introduction

The self-assembly of well-defined coordination architectures from well-designed organic ligands and specific metal ions is directed by the steric information of the ligands and the coordination algorithm of the metal ion.[1] Until now, great efforts have been made to determine the relationship between the number, type, and spatial disposition of binding sites on the ligand, the stereoelectronic preferences of the metal ion, and the structures of complexes, as well as the relationship between structures and physical properties, such as cavities/porousness of the metal–organic framework and magnetic and luminescent characteristics.[2] However, there is still not a general method to achieve the tailoring construction of systems with expected structures and properties.[3]

In recent years, the magneto–structural correlations have been attracting great interest, not only in the theory of magnetism but also in exploiting magnetic materials.[4] In the

---

* To whom correspondence should be addressed. E-mail: buxh@nankai.edu.cn. Fax: +86-22-23502458. Tel: +86-22-23502809.

[†] Nankai University.

[‡] Universitat de Barcelona.

(1) For examples: (a) Baxter, P. N. W.; Lehn, J.-M.; Fischer, J.; Youinou, M.-T. *Angew. Chem., Int. Ed. Engl.* **1994**, *33*, 2284. (b) Smith, V. C. M.; Lehn, J.-M. *Chem. Commun.* **1996**, 2320. (c) Smith, V. C. M.; Lehn, J.-M. *Chem. Commun.* **1996**, 2733. (d) Hasenknopf, B.; Lehn, J.-M.; Boumediene, N.; Dupont-Gervais, A.; Van Dorsselaer, A.; Kneisel, B.; Fenske, D. *J. Am. Chem. Soc.* **1997**, *119*, 10956. (e) Barboiu, M.; Vaughan, G.; Graff, R.; Lehn, J.-M. *J. Am. Chem. Soc.* **2003**, *125*, 10257.

(2) For examples: (a) Beissel, T.; Powers, R. E.; Raymond, K. N. *Angew. Chem., Int. Ed.* **1996**, *35*, 1084. (b) Mann, K. L. V.; Psillakis, E.; Jeggry, J. C.; Rees, L. H.; Harden, N. M.; McCleverty, J. A.; Ward, M. D.; Gatteschi, D.; Totti, F.; Mabbs, F. E.; McInnes, E. J. L.; Riedi, P. C.; Smith, G. M. *J. Chem. Soc., Dalton Trans.* **1999**, 339. (c) Eddaoudi, M.; Kim, J.; Wachter, J. B.; Chae, H. K.; O’Keeffe, M.; Yaghi, O. M. *J. Am. Chem. Soc.* **2001**, *123*, 4368. (d) Marvin, C.; Charton, B. I. *Advances in Quantitative Structure-Property Relationships*; JAI Press: Amsterdam, 2002. (e) Bunzli, J.-C. G.; Piguet, C. *Chem. Rev.* **2002**, *102*, 1897. (f) Poulsen, R. D.; Bentien, A.; Chevalier, M.; Iversen, B. B. *J. Am. Chem. Soc.* **2005**, *127*, 9156.

10.1021/ic051488d CCC: $33.50

© 2006 American Chemical Society
Published on Web 12/07/2005

Chart 1

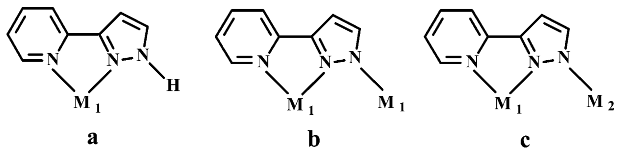

magnetism researches of metal−organic complexes, Cu^{II} is widely explored, because it is well-known to produce variable and distorted coordination geometries and have a simple electronic configuration.[5] On the other hand, the selection of organic ligands is very pivotal for obtaining multinuclear magnetic coupling system. There are many reports on the magnetic properties of complexes with pyrazole-based ligands and Cu^{II} centers.[6] For example, a novel two-dimensional (2-D) Cu^{II} complex, with the ligand 3,5-pyrazoledicarboxylic acid, and its magnetic properties have been reported.[6b] It is interesting that there are different magnetic behaviors between Cu^{II} centers at different temperatures, due to the effect of the bridging groups (pyrazolate and carboxylate bridges). In general, in the magnetism, the complexes with pyrazole-based ligands show very strong antiferromagnetic coupling.

3-(2-Pyridyl)pyrazole ($H\mathbf{L}^1$), first reported by Tisler and co-workers[7] in 1980, is a multifunctional ligand having several coordination modes. For a long time, $H\mathbf{L}^1$ was just considered as a simple bidentate chelate ligand[8] similar to 2,2′-bipyridine (Chart 1a) until 1996, when Ward and co-workers[9] observed another coordination mode, acting as a terdentate bridging ligand via deprotonation of the pyrazoly NH group and coordination of the pyrazolyl N atom to a second metal ion (Chart 1b). Later, Lam and co-workers[10] synthesized a triple-stranded helical complex, $[(Ru\mathbf{L}^1_3)_2Cu_3](ClO_4)$, in which $\mathbf{L}^1$ is a terdentate ligand bridging two different metal centers (Chart 1c). Heretofore, the coordination chemistry of $H\mathbf{L}^1$ with some first-row transition metal ions, Fe^{II},[8,11] Fe^{III},[9] Cu^{I},[12] Ni^{II},[2b,8] and Zn^{II},[2b] has been studied by several researchers. However, to the best of our knowledge, only two structurally related Cu^{II} complexes with $\mathbf{L}^1$, $[Cu_4(\mathbf{L}^1)_6(DMF)_2][PF_6]_2$ (**8**)[2b,13] and $[Cu_4(\mathbf{L}^1)_6(MeOH)_2][PF_6]_2$ (**9**),[2b] have been reported to date.

As a systematic investigation of the coordination chemistry of $H\mathbf{L}^1$ with Cu^{II}, herein, we describe the designed preparation, structural characterization, and magnetic properties of seven new Cu^{II} complexes with $H\mathbf{L}^1$, ranging from dinuclear to tetranuclear and then to a 1-D chain: $[Cu(\mu\text{-}\mathbf{L}^1)(NO_3)(H_2O)]_2$ (**1**), $[Cu(\mu\text{-}\mathbf{L}^1)(H\mathbf{L}^1)(ClO_4)]_2$ (**2**), $[Cu_4(\mu\text{-}\mathbf{L}^1)_6(NO_3)_2]$ (**3**), $[Cu_4(\mu\text{-}\mathbf{L}^1)_6(\mathbf{L}^1)_2]$ (**4**), $[Cu_4(\mu\text{-}\mathbf{L}^1)_6(\mu\text{-}\mathbf{L}^2)]_n$ (**5**), $[Cu_4(\mu\text{-}\mathbf{L}^1)_6(\mu\text{-}\mathbf{L}^3)]_n$ (**6**), and $\{[Cu_4(\mu\text{-}\mathbf{L}^1)_4(\mu\text{-}\mathbf{L}^4)_2](H_2O)_3\}_n$ (**7**) ($H\mathbf{L}^1$ = 3-(2-pyridyl)pyrazole, $\mathbf{L}^2$ = 1,8-naphthalenedicarboxylate, $\mathbf{L}^3$ = terephthalate, $\mathbf{L}^4$ = 2,6-pyridinedicarboxylate). The magnetic properties of all the complexes were investigated, and a systematic magneto−structural correlation has been discussed in detail.

Experimental Section

Materials and General Methods. All the solvents and reagents for synthesis were commercially available and used as received. 3-(2-Pyridyl)pyrazole ($H\mathbf{L}^1$) was synthesized according to a literature method.[14] $Cu(ClO_4)_2$ was prepared according to a literature method.[15] IR spectra were measured on a TENSOR 27 (Bruker) FT-IR spectrometer with KBr pellets in the range 4000−400 cm^{-1}. Elemental analyses of C, H, and N were performed on a Perkin-Elmer 240C analyzer.

Synthesis of Complexes. $[Cu(\mu\text{-}L^1)(NO_3)(H_2O)]_2$ (1). Single crystals suitable for X-ray analysis for **1** were obtained by the following method: To a colorless solution of $H\mathbf{L}^1$ (0.2 mmol) dissolved in anhydrous EtOH (15 mL) was added $Cu(NO_3)_2\cdot 3H_2O$ (0.2 mmol) under stirring for a few minutes. The solution was then filtered and left to stand at room temperature. Blue single crystals were obtained after 2 days with the solvent evaporation. Yield: ~60%. Anal. Calcd for $C_{16}H_{16}Cu_2N_8O_8$: C, 33.40; H, 2.80; N, 19.47. Found: C, 33.01; H, 2.63; N, 19.58. IR (cm^{-1}): 3493 m, 1614 m, 1569 w, 1492 vs, 1455 m, 1434 m, 1384 m, 1359 m, 1286 s, 1155 s, 1135 m, 1096 w, 1008 s, 951 w, 804 m, 776 s, 710 m, 513 w, 418 w.

$[Cu(\mu\text{-}L^1)(HL^1)(ClO_4)]_2$ (2). Blue single crystals of **2** suitable for X-ray analysis were obtained by a similar method used for **1**,

---

(3) For examples: (a) Jung, O.-S.; Kim, Y. J.; Lee, Y.-A.; Chae, H. K.; Jang, H. G.; Hong, J. *Inorg. Chem.* **2001**, *40*, 2105. (b) Li, J. R.; Zhang, R. H.; Bu, X. H. *Cryst. Growth Des.* **2003**, *3*, 829. (c) Steel, P. J. *Acc. Chem. Res.* **2005**, *38*, 243. (d) Han, Z.-B.; Cheng, X.-N.; Chen, X.-M. *Cryst. Growth Des.* **2005**, *5*, 695.

(4) For examples: (a) Monfort, M.; Resino, I.; Ribas, J.; Solans, X.; Font-Bardia, M.; Rabu, P.; Drillon, M. *Inorg. Chem.* **2000**, *39*, 2572. (b) Gutschke, S. O. H.; Price, D. J.; Powell, A. K.; Wood, P. T. *Angew. Chem., Int. Ed.* **2001**, *113*, 1974. (c) Du, M.; Guo, Y. M.; Bu, X. H.; Ribas, J.; Monfort, M. *New J. Chem.* **2002**, *5*, 645. (d) Yoon, J.; Mirica, L. M.; Stack, T. D. P.; Solomon, E. I. *J. Am. Chem. Soc.* **2004**, *126*, 12586. (e) Zhao, M.; Zhong, C.; Stern, C.; Barrett, A. G. M.; Hoffman, B. M. *J. Am. Chem. Soc.* **2005**, *127*, 9769. (f) Triki, S.; Gomez-Garcia, C. J.; Ruiz, E.; Sala-Pala, J. *Inorg. Chem.* **2005**, *44*, 5501.

(5) For examples: (a) Triki, S.; Pala, J. S.; Decoster, M.; Molinié, P.; Toupet, L. *Angew. Chem., Int. Ed.* **1999**, *38*, 113. (b) Plass, W.; Pohlmann, A.; Rautengarten, J. *Angew. Chem., Int. Ed.* **2001**, *40*, 4207. (c) Cao, R.; Shi, Q.; Sun, D. F.; Hong, M. C.; Bi, W. H.; Zhao, Y. J. *Inorg. Chem.* **2002**, *41*, 6161. (d) Du, M.; Guo, Y. M.; Chen, S. T.; Bu, X. H.; Batten, S. R.; Ribas, J.; Kitagawa, S. *Inorg. Chem.* **2004**, *43*, 1287. (e) Talukder, P.; Datta, A.; Mitra, S.; Rosair, G.; El Fallah, M. S.; Ribas, J. *J. Chem. Soc., Dalton Trans.* **2004**, 4161. (f) You, Y. S.; Yoon, J. H.; Kim, H. C.; Hong, C. S. *Chem. Commun.* **2005**, 4116.

(6) (a) Du, M.; Chen, S.-T.; Guo, Y.-M.; Bu, X.-H.; Ribas, J. *J. Mol. Struct.* **2005**, *737*, 17 and references therein. (b) King, P.; Clérac, R.; Anson, C. E.; Coulon, C.; Powell, A. K. *Inorg. Chem.* **2003**, *42*, 3492 and references therein. (c) Escuer, A.; Vicente, R.; Mernari, B.; El Gueddi, A.; Pierrot, M. *Inorg. Chem.* **1997**, *36*, 2511 and references therein. (d) Abraham, F.; Lagrenee, M.; Sueur, S.; Mernari, B.; Bremard, C. *J. Chem. Soc., Dalton Trans.* **1991**, 1443.

(7) Tisler, M.; Stanovnik, B.; Versek, B. *Vestn. Slov. Kem. Drus.* **1980**, *27*, 65.

(8) Sugiyarto, K. H.; Goodwin, H. A. *Aust. J. Chem.* **1988**, *41*, 1645.

(9) Jones, P. L.; Jeffery, J. C.; McCleverty, J. A.; Ward, M. D. *Polyhedron* **1997**, *16*, 1567.

(10) Lam, M. H. W.; Cheung, S. T. C.; Fung, K.-M.; Wong, W.-T. *Inorg. Chem.* **1997**, *36*, 4618.

(11) (a) Harimanow, L. S.; Sugiyarto, K. H.; Craig, M. L.; Goodwin, H. A. *Aust. J. Chem.* **1999**, *52*, 109. (b) Leita, B. A.; Moubaraki, B.; Murray, K. S.; Smith, J. P.; Cashion, J. D. *Chem. Commun.* **2004**, 156.

(12) Singh, K.; Long, J. R.; Stavropoulos, P. *J. Am. Chem. Soc.* **1997**, *119*, 2942.

(13) Jeggry, J. C.; Jones, P. L.; Mann, K. L. V.; Psillakis, E.; McCleverty, J. A.; Ward, M. D. *Chem. Commun.* **1997**, 175.

(14) (a) Brunner, H.; Scheck, T. *Chem. Ber.* **1992**, *125*, 701. (b) Amoroso, A. J.; Cargill Thompson, M. W.; Jeffery, J. C.; Jones, P. L.; McCleverty, J. A.; Ward, M. D. *Chem. Commun.* **1994**, 2751. (c) Wang, F.; Schwabacher, A. W. *Tetrahedron Lett.* **1999**, *40*, 4779.

(15) (a) Pascal, J. L.; Potier, J.; Jones, D. J.; Roziere, J.; Michalowicz, A. *Inorg. Chem.* **1984**, *23*, 2068. (b) Jansen, M.; Tobias, K. M. *Angew. Chem., Int. Ed. Engl.* **1986**, *25*, 993.

with $Cu(ClO_4)_2$ instead of $Cu(NO_3)_2{\cdot}3H_2O$. Yield: ∼60%. Anal. Calcd for $C_{32}H_{26}Cl_2Cu_2N_{12}O_8$: C, 42.49; H, 2.90; N, 18.58. Found: C, 42.18; H, 2.54; N, 18.93. IR (cm^{-1}): 3204 b, 3040 m, 2974 m, 1613 s, 1570 m, 1540 w, 1474 m, 1459 m, 1433 s, 1362 m, 1289 w, 1256 w, 1219 m, 1154 s, 1106 vs, 1078 vs, 1058 v, 969 m, 950 w, 930 w, 798 w, 765 s, 712 m, 625 s, 509 w.

[$Cu_4(\mu$-$L^1)_6(NO_3)_2$] (3). Complex **3** was obtained by the reaction of $Cu(NO_3)_2{\cdot}3H_2O$ and H**L**^{1} in the molar ratio of 2:3 mixed with 15 mL of water under hydrothermal conditions at 140 °C for 2 days. The blue crystals were washed by water and acetone and dried in air. Yield: ∼35%. Anal. Calcd for $C_{48}H_{36}Cu_4N_{20}O_6$: C, 46.38; H, 2.92; N, 22.53. Found: C, 46.20; H, 2.58; N, 22.97. IR (cm^{-1}): 1613 s, 1596 m, 1568 w, 1523 w, 1459 m, 1434 s, 1403 s, 1385 s, 1361 m, 1311 vs, 1141 s, 1097 m, 1038 w, 950 w, 755 vs, 711 w, 640 w, 512 w, 415 w.

[$Cu_4(\mu$-$L^1)_6L^1{}_2$] (4). The dark blue crystals of complex **4** were obtained by the reaction of $Cu(NO_3)_2{\cdot}3H_2O$, H**L**^{1}, and NaOH in the molar ratio of 1:2:2 mixed with 15 mL of water under hydrothermal conditions at 140 °C for 2 days. Yield: ∼50%. Anal. Calcd for $C_{64}H_{48}Cu_4N_{24}$: C, 54.62; H, 3.44; N, 23.88. Found: C, 54.13; H, 3.23; N, 24.02. IR (cm^{-1}): 1606 s, 1594 s, 1565 m, 1524 m, 1452 s, 1359 m, 1338 m, 1276 w, 1152 m, 1133 m, 1099 w, 1075 w, 1002 w, 985 w, 949 w, 934 w, 785 m, 750 s, 711 w, 643 w, 503 w, 411 w.

[$Cu_4(\mu$-$L^1)_6(\mu$-$L^2)]_n$ (5), [$Cu_4(\mu$-$L^1)_6(\mu$-$L^3)]_n$ (6), and {[$Cu_4(\mu$-$L^1)_4(\mu$-$L^4)_2](H_2O)_3\}_n$ (7). Complexes **5**−**7** were synthesized by the reaction of $Cu(NO_3)_2{\cdot}3H_2O$, H**L**^{1}, 1,8-naphthalenedicarboxylic acid (for **5**), terephthalic acid (for **6**), or pyridinedicarboxylic acid (for **7**), and NaOH in the molar ratio of 4:6:1:8 mixed with 15 mL of water under hydrothermal conditions at 140°C for 2 days. For **5**, navy blue crystals formed, yield: ∼40%. Anal. Calcd for $C_{30}H_{21}Cu_2N_9O_2$: C, 54.05; H, 3.18; N, 18.91. Found: C, 53.90; H, 3.21; N, 18.55. IR (KBr, cm^{-1}): 1620 s, 1608 vs, 1598 vs, 1566 m, 1455 m, 1433 w, 1385 w, 1353 m, 1340 m, 1220 w, 1146 m, 1098 w, 1079 w, 1017 w, 1005 w, 977 w, 950 w, 778 m, 763 s, 710 w, 685 w, 643 w, 505 w. For **6**, deep blue crystals formed, yield: ∼50%. Anal. Calcd for $C_{28}H_{20}Cu_2N_9O_2$: C, 52.42; H, 3.14; N, 19.65. Found: C, 52.13; H, 3.21; N, 19.31. IR (cm^{-1}): 1611 m, 1593 m, 1565 w, 1452 m, 1431 m, 1397 w, 1355 s, 1148 m, 1095 w, 1074 w, 1016 w, 986 w, 943 w, 822 w, 788 w, 760 s, 745 w, 711 w, 643 w, 504 w. For **7**, deep blue crystals formed, yield: ∼60%. Anal. Calcd for $C_{46}H_{36}Cu_4N_{14}O_{11}$: C, 45.47; H, 2.99; N, 16.14. Found: C, 45.09; H, 2.55; N, 16.53. IR (cm^{-1}): 3440 m, 1634 vs, 1586 s, 1476 m, 1458 s, 1433 s, 1381 s, 1361 vs, 1275 m, 1189 w, 1153 s, 1099 m, 1078 m, 1017 w, 994 w, 952 w, 906 m, 867 w, 769 s, 715 m, 699 w, 665 w, 642 w, 511 w, 415 m.

Caution! *Perchlorate complexes of metal ions in the presence of organic ligands are potentially explosive. Only a small amount of material should be used and handled with care.*

X-ray Data Collection and Structure Determinations. X-ray single-crystal diffraction data for complexes **1**−**7** were collected on a Bruker Smart 1000 CCD diffractometer at 293(2) K with Mo Kα radiation ($\lambda = 0.710\ 73$ Å) by the ω-scan mode. The program SAINT[16] was used for integration of the diffraction profiles. All the structures were solved by direct methods using the SHELXS program of the SHELXTL package and refined by full-matrix least-squares methods with SHELXL (semiempirical absorption corrections were applied using the SADABS program).[17] Metal atoms in each complex were located from the *E*-maps, and other non-hydrogen atoms were located in successive difference Fourier syntheses and refined with anisotropic thermal parameters on F^2. The hydrogen atoms of the ligands were generated theoretically onto the specific atoms and refined isotropically with fixed thermal factors. The hydrogens of coordinated water molecules in **1** were added by difference Fourier maps, and those of the packing water molecules in **7** were not added. Further details for structural analysis are summarized in Table 1.

Magnetic Measurements. The variable-temperature magnetic susceptibilities were measured in "Servei de Magnetoquímica (Universitat de Barcelona)" on polycrystalline samples (ca. 30 mg) with a Quantum Design MPMS SQUID magnetometer operating at a magnetic field of 0.1 T between 2 and 300 K. All data were corrected for diamagnetism estimated from Pascal's constants. EPR spectra were recorded at room temperature on powder samples at X-band frequency with a Bruker 300E automatic spectrometer.

Results and Discussion

Synthesis Consideration and General Characterization. The designed syntheses of all complexes are mainly based on the following considerations: (1) H**L**^{1} has several coordination modes, and the one adopted in the complex formation is related to the reaction conditions. (2) The Cu^{II} ion has several coordination geometries, which affect the magnetic properties of its complexes. (3) The introduction of the second ligand may extend a low-dimensional structure to a higher one. (4) Due to the diverse coordination modes of the ligand and Cu^{II} ion, under different conditions, such as normal solution system and hydrothermal conditions, different complexes may be obtained.

Complex **1**, [$Cu(\mu$-$L^1)(NO_3)(H_2O)]_2$, was prepared by the reaction of $Cu(NO_3)_2{\cdot}3H_2O$ with H**L**^{1} in anhydrous ethanol at room temperature. In **1**, the ratio of metal and **L**^{1} is 2:2, in which H**L**^{1} acts as a terdentate chelating/bridging ligand via deprotonation of the pyrazole NH group. Apparently, this coordination mode is different from that of the same ligands with other first-row transition metal ions Zn^{II}[2b] and Ni^{II}[2b,8] in which H**L**^{1} is just a simple bidentate chelating ligand. The Cu^{II} center is coordinated to two oxygen atoms of one water molecule and one nitrate anion to fulfill the stereochemical requirements of the metal. To investigate whether H**L**^{1} can fulfill the stereochemical requirements of Cu^{II} ion, the reaction of H**L**^{1} with $Cu(ClO_4)_2$ instead of $Cu(NO_3)_2{\cdot}3H_2O$ under the same conditions with those of **1** simultaneously can exclude the coordination of nitrate anions and water molecules, gave rise to a dinuclear complex **2**, [$Cu(\mu$-$L^1)(HL^1)(ClO_4)]_2$, in which H**L**^{1} acts as both simple bidentate chelating ligand and terdentate chelating/bridging ligand. In **2**, there are two simple bidentate chelating ligands H**L**^{1} which also have the capacity to act as terdentate ligands. Then we synthesized **3**, [$Cu_4(\mu$-$L^1)_6(NO_3)_2$], and **4**, [$Cu_4(\mu$-$L^1)_6L^1{}_2$], by hydrothermal conditions. In a comparison of **3** and **4** with **8**[2b,13] and **9**,[2b] the two nitrate anions coordinated to Cu2 and Cu2A in **3** and the two bidentate chelating ligand **L**^{1} coordinated to Cu2 and Cu2A in **4** are easily substituted by other anion ligands, retaining the gridlike structure of the tetranuclear Cu^{II}. Thus, the gridlike structure of the tetranuclear Cu^{II} was bridged by dicarboxylate (terephthalate and 1,8-naphthalenedicarboxylate) to obtain 1-D complexes, [Cu_4-

---

(16) *SAINT Software Reference Manual*; Bruker AXS: Madison, WI, 1998.

(17) Sheldrick, G. M. *SHELXTL NT Version 5.1. Program for Solution and Refinement of Crystal Structures*; University of Göttingen: Göttingen, Germany, 1997.

Table 1. Crystal Data and Structure Refinement Parameters for Complexes **1**−**7**

param	**1**	**2**	**3**	**4**
chem formula	$C_{16}H_{16}Cu_2N_8O_8$	$C_{32}H_{26}Cu_2Cl_2N_{12}O_8$	$C_{48}H_{36}Cu_4N_{20}O_6$	$C_{64}H_{48}Cu_4N_{24}$
fw	575.45	904.63	1243.13	1407.42
space group	$P\bar{1}$	$P\bar{1}$	$P2_1/c$	$P2_1/c$
a (Å)	7.314(1)	8.773(3)	10.398(2)	12.884(3)
b (Å)	8.500(2)	10.250(4)	21.386(3)	18.068(4)
c (Å)	9.2998(2)	11.198(4)	10.870(2)	12.618(3)
α (deg)	112.946(3)	74.796(6)	90	90
β (deg)	91.242(3)	70.617(6)	95.392(2)	103.291(4)
γ (deg)	100.638(3)	80.120(6)	90	90
V (Å^3)	520.43(2)	912.6(6)	2406.6(6)	2858.5(1)
Z	1	1	2	2
D (g cm^{-3})	1.836	1.646	1.716	1.635
μ (mm^{-1})	2.108	1.380	1.818	1.536
T (K)	293(2)	293(2)	293(2)	293(2)
R^a/R_w^b	0.0304/0.0756	0.0498/0.1066	0.0337/0.0779	0.0666/0.1160

param	**5**	**6**	**7**
chem formula	$C_{30}H_{21}Cu_2N_9O_2$	$C_{28}H_{20}Cu_2N_9O_2$	$C_{46}H_{36}Cu_4N_{14}O_{11}$
fw	666.64	641.61	1215.06
space group	$C2/c$	$P2_1/n$	$P\bar{1}$
a (Å)	19.674(6)	12.112(3)	8.348(2)
b (Å)	12.787(4)	12.420(3)	12.348(3)
c (Å)	21.570(7)	19.217(4)	23.053(5)
α (deg)	90	90	87.232(4)
β (deg)	97.964(5)	104.611(4)	81.369(4)
γ (deg)	90	90	84.222(4)
V (Å^3)	5374(3)	2797.2(1)	2336.0(9)
Z	8	4	2
D (g cm^{-3})	1.648	1.524	1.719
μ (mm^{-1})	1.631	1.564	1.875
T (K)	293(2)	293(2)	293(2)
R^a/R_w^b	0.0606/0.1152	0.0551/0.1021	0.0697/0.1370

^{a} $R = \Sigma||F_o| - |F_c||/\Sigma|F_o|$. ^{b} $R_w = [\Sigma[w(F_o^2 - F_c^2)^2]/\Sigma w(F_o^2)^2]^{1/2}$.

$(\mu\text{-}\mathbf{L}^1)_6(\mu\text{-}\mathbf{L}^2)]_n$ (**5**) and $[Cu_4(\mu\text{-}\mathbf{L}^1)_6(\mu\text{-}\mathbf{L}^3)]_n$ (**6**). The 1-D chain complex $\{[Cu_4(\mu\text{-}\mathbf{L}^1)_4(\mu\text{-}\mathbf{L}^4)_2](H_2O)_3\}_n$ (**7**) was obtained when pyridinedicarboxylic acid was used instead of 1,8-naphthalenedicarboxylic acid and terephthalic acid.

The IR spectra of all the seven complexes show absorption bands resulting from the skeletal vibrations of the aromatic rings in the 1400−1615 cm^{-1} range. In the IR spectra of **1** and **7**, the broad band centered at ca. 3450 cm^{-1} indicates the O−H stretching of the aqua molecules. For the existences of the NO_3^- anion, the IR spectra of **1** and **3** show strong absorption bands at ∼1385 and ∼765 cm^{-1}. For **2**, the occurrence of split ν_{Cl-O} stretches of the ClO_4^- anions at ∼1100 cm^{-1} provides good evidence of their involvement in the formation of hydrogen bonding, and the broad band at 3204 cm^{-1} indicates the N−H stretching of H$\mathbf{L}^1$. For **5**−**7**, the IR spectra display the characteristic bands of the carboxylate anions at ∼1620 and ∼1600 cm^{-1} for $\nu_{asym(C-O)}$, ∼1375 and ∼1350 cm^{-1} for $\nu_{sym(C-O)}$, and ∼765 cm^{-1} for $\delta_{(O-C-O)}$. The $\Delta(\nu_{as}-\nu_{sym})$ values indicate that the carboxylate anions coordinate to the Cu^{II} center in monodendate mode, which is consistent with the crystal structure as described later.

Structure Descriptions of Complexes 1−7. $[Cu(\mu\text{-}L^1)(NO_3)(H_2O)]_2$ (1). The molecular structure of the centrosymmetric neutral dinuclear complex **1** is shown in Figure 1a. The Cu^{II} ion is pentacoordinated to three nitrogen atoms (one pyridine N and two pyrazole N) of two distinct $\mathbf{L}^1$ ligands (Cu−N lengths being 1.953(2)−2.025(2) Å), one oxygen atom of nitrate anion (Cu−O = 2.066(2) Å), and one oxygen atom from the coordinated water molecule (Cu−O = 2.253(2) Å) to form a square-pyramid geometry. The Cu^{II} center deviates from the mean equatorial plane defined by three coordinated nitrogen atoms and one oxygen atom from nitrate anion toward the apical O1w by 0.157 Å. The selected bond distances and angles are listed in Table 2. In **1**, two $\mathbf{L}^1$ ligands bridge two Cu^{II} ions to form an approximately planar $[Cu(\mu\text{-}\mathbf{L}^1)]_2$ binuclear structure containing a six-membered ring, (Cu−N−N−)$_2$, in which, the Cu⋯Cu distance is 3.920 Å. The coordinated water molecules and nitrate anions lie on the periphery of the plane, up and down, respectively. Each $\mathbf{L}^1$ ligand plays two types of roles, chelating one Cu^{II} center and simultaneously bridging the other one, showing a terdenate chelating−bridging mode.

In the crystal net, as shown in Figure 1b, the neutral molecules of **1** are bound together by strong intermolecular hydrogen bonds to create a 1-D chain motif expanding along the crystallographic c axis. The hydrogen-bonding system in **1** consists of the coordinated oxygen atom, O1, on the NO_3^- group with the hydrogen atom H1wA on the coordinated water molecule O1w of a neighboring molecule. The O1⋯H1wA distance is 2.052 Å, the corresponding O1w⋯O1 distance is 2.852 Å, and the O1w−H1wA⋯O1 angle is 168.7°. It is no doubt that these strong hydrogen-bonding interactions contribute significantly to the alignment of the molecules of **1** in the crystalline state. In addition, as shown in Figure 1c, the intermolecular $\pi-\pi$ stackings further assemble the above-mentioned hydrogen-bonded chains to form a 3-D supramolecular framework. The interplanar

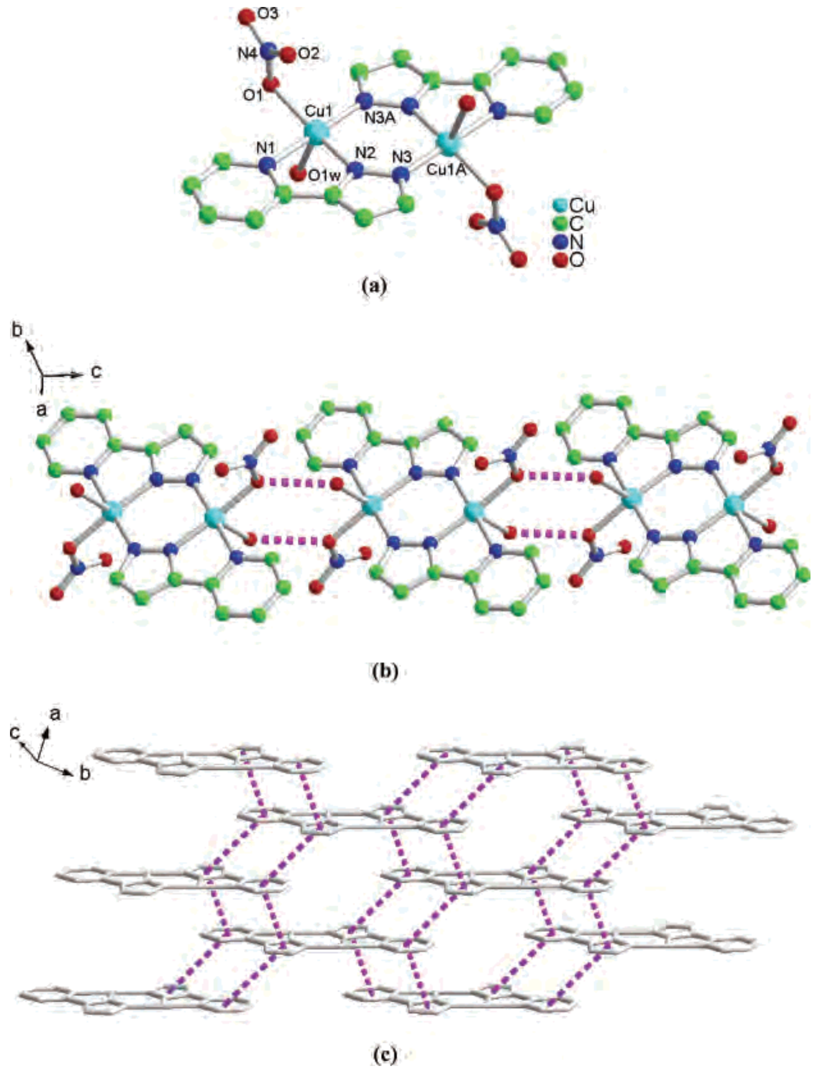

Figure 1. (a) Molecular structure of the dinuclear complex **1**. (b) Infinite quasi 1-D structure formed through H-bonds in **1**. (c) View of the face-to-face $\pi-\pi$ stacking interactions in **1**.

Table 2. Selected Bond Distances (Å) and Angles (deg) for Complex $\mathbf{1}^a$

Cu(1)−N(1)	2.025(2)	Cu(1)−N(2)	1.965(2)
Cu(1)−N(3)$^{\#1}$	1.953(2)	Cu(1)−O(1)	2.066(2)
Cu(1)−O(1W)	2.253(2)		
N(3)$^{\#1}$−Cu(1)−N(2)	98.06(8)	N(3)$^{\#1}$−Cu(1)−N(1)	178.81(8)
N(2)−Cu(1)−N(1)	81.16(8)	N(3)$^{\#1}$−Cu(1)−O(1)	89.09(8)
N(2)−Cu(1)−O(1)	161.55(8)	N(1)−Cu(1)−O(1)	91.39(8)
N(3)$^{\#1}$−Cu(1)−O(1W)	90.93(9)	N(2)−Cu(1)−O(1W)	109.12(9)
N(1)−Cu(1)−O(1W)	90.18(9)	O(1)−Cu(1)−O(1W)	87.62(8)

^{a} Symmetry code: (#1) $-x + 1$, $-y + 1$, $-z + 2$.

distances between neighboring parallel aromatic rings of $\mathbf{L}^1$ are ca. 3.4 and 3.5 Å, indicating the presence of face-to-face $\pi-\pi$ stacking interactions that further stabilize the crystal structure.[18]

[Cu(μ-L^1)(HL^1)(ClO$_4$)]$_2$ (2). Similar to that of **1**, complex **2** also has a centrosymmetric dinuclear structure (Figure 2a), in which the Cu$^{\mathrm{II}}$ center is coordinated to five nitrogen atoms, three from two $\mathbf{L}^1$ and two from one H**L**, and one oxygen atom of perchlorate anion. The important bond lengths and angles are listed in Table 3. The distance between the Cu$^{\mathrm{II}}$ center and the perchlorate oxygen atom (O2) is 2.723 Å, being considered as a weak coordination. Thus, the coordination geometry of the Cu$^{\mathrm{II}}$ ion can be described as a distorted octahedron (for the related bond angles, see Table 3). As that in **1**, in **2** two $\mathbf{L}^1$ ligands bridge two Cu$^{\mathrm{II}}$ centers to form a planar [Cu(μ-$\mathbf{L}^1$)]$_2$ binuclear unit, related by an inversion center, in which each $\mathbf{L}^1$ acts as a terdentate chelating−bridging linkage. The Cu···Cu distance is 3.920 Å, being the same as that of **1**. Different from **1**, in the structure of **2** a neutral H$\mathbf{L}^1$ molecule coordinated to each Cu$^{\mathrm{II}}$ center is in a chelating coordination mode. The hydrogen atom of H$\mathbf{L}^1$ hydrogen bonds to the O1 atom of a perchlorate anion, with the O1···H distance of 2.042 Å and O1···N6 of 2.870 Å. The coexistence of **L** and H**L** in the same complex is interesting in this system and shows that the H**L** has various coordination characters. Indeed, the structure of this complex is more similar to that of [Fe(μ-$\mathbf{L}^1$)(H$\mathbf{L}^1$)(NCSe)]$_2$,[11b] with only different cocoordinated anions. In addition, in the crystal structure of **2**, there exists the intermolecular $\pi-\pi$ stackings between $\mathbf{L}^1$ ligands. The $\mathbf{L}^1$ planes of neighboring complex

---

(18) (a) Munakata, M.; Wu, L. P.; Yamamoto, M.; Kuroda-Sowa, T.; Maekawa, M. *J. Am. Chem. Soc.* **1996**, *118*, 3117. (b) Sugimori, T.; Masuda, H.; Ohata, N.; Koiwai, K.; Odani, A.; Yamauchi, O. *Inorg. Chem.* **1997**, *36*, 576.

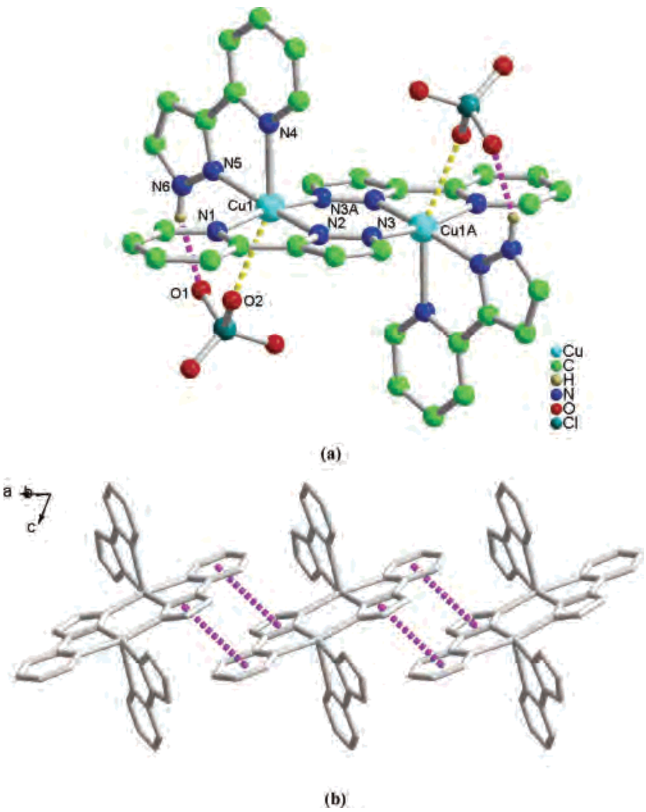

Figure 2. (a) Molecular structure of the dinuclear complex **2**. (b) Infinite quasi 1-D chain structure formed through the face-to-face $\pi-\pi$ stacking interactions in **2**.

Table 3. Selected Bond Distances (Å) and Angles (deg) for Complex $\mathbf{2}^a$

Cu(1)−N(1)	2.042(3)	Cu(1)−N(2)	1.965(3)
Cu(1)−N(3)$^{\#1}$	1.969(3)	Cu(1)−N(4)	2.298(3)
Cu(1)−N(5)	2.027(3)		
N(2)−Cu(1)−N(3)$^{\#1}$	97.72(1)	N(2)−Cu(1)−N(5)	167.59(1)
N(3)$^{\#1}$−Cu(1)−N(5)	91.81(1)	N(2)−Cu(1)−N(1)	81.08(1)
N(3)$^{\#1}$−Cu(1)−N(1)	169.49(1)	N(5)−Cu(1)−N(1)	90.96(1)
N(2)−Cu(1)−N(4)	95.30(1)	N(3)$^{\#1}$−Cu(1)−N(4)	99.43(1)
N(5)−Cu(1)−N(4)	75.22(1)	N(1)−Cu(1)−N(4)	91.07(1)

[a] Symmetry code: (#1) $-x + 1, -y + 2, -z + 1$.

molecules are almost parallel with each other, and the interplanar distance is ca. 3.4 Å. As shown in Figure 2b, such $\pi-\pi$ interactions extend the dinuclear molecule to form a 1-D supramolecular chain along the crystallographic *a* axis.

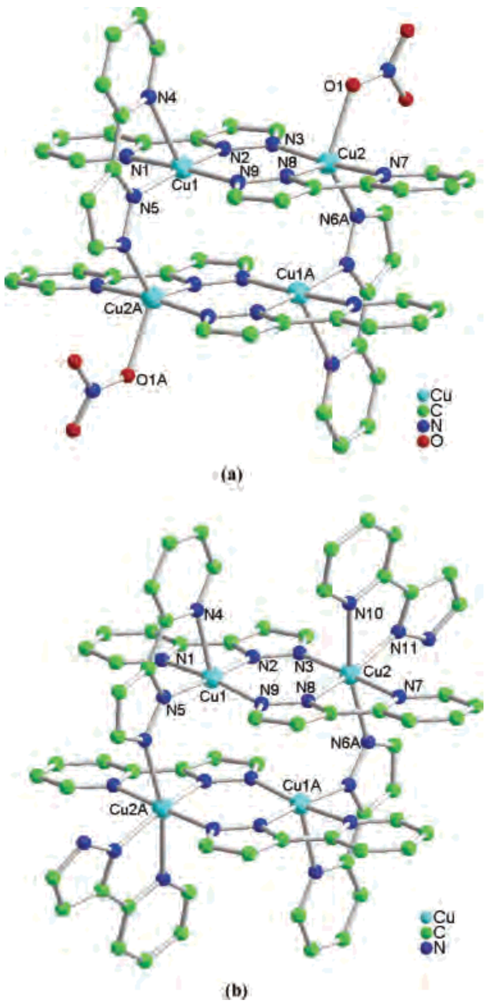

Figure 3. Molecular structures of the tetranuclear complexes (a) **3** and (b) **4**.

Table 4. Selected Bond Distances (Å) and Angles (deg) for Complex $\mathbf{3}^a$

Cu(1)−N(2)	1.970(2)	Cu(1)−N(5)	1.973(2)
Cu(1)−N(9)	1.977(2)	Cu(1)−N(1)	2.063(2)
Cu(1)−N(4)	2.448(2)	Cu(2)−N(3)	1.949(2)
Cu(2)−N(8)	1.984(2)	Cu(2)−N(7)	2.018(2)
Cu(2)−N(6)$^{\#1}$	2.062(2)	Cu(2)−O(1)	2.188(1)
N(2)−Cu(1)−N(5)	167.98(9)	N(2)−Cu(1)−N(9)	97.24(8)
N(5)−Cu(1)−N(9)	90.27(8)	N(2)−Cu(1)−N(1)	80.06(8)
N(5)−Cu(1)−N(1)	91.78(8)	N(9)−Cu(1)−N(1)	175.29(8)
N(2)−Cu(1)−N(4)	114.24(8)	N(5)−Cu(1)−N(4)	74.07(8)
N(9)−Cu(1)−N(4)	95.84(8)	N(1)−Cu(1)−N(4)	88.80(8)
N(3)−Cu(2)−N(8)	96.58(8)	N(3)−Cu(2)−N(7)	173.19(9)
N(8)−Cu(2)−N(7)	80.84(9)	N(3)−Cu(2)−N(6)$^{\#1}$	95.25(9)
N(8)−Cu(2)−N(6)$^{\#1}$	125.94(8)	N(7)−Cu(2)−N(6)$^{\#1}$	91.34(9)
N(3)−Cu(2)−O(1)	90.2(2)	N(8)−Cu(2)−O(1)	108.4(5)
N(7)−Cu(2)−O(1)	84.7(2)	N(6)$^{\#1}$−Cu(2)−O(1)	124.1(4)

[a] Symmetry operations: (#1) $-x + 1, -y + 1, -z + 2$.

$[Cu_4(\mu\text{-}L^1)_6(NO_3)_2]$ (3). Complex **3** has a centrosymmetric tetranuclear gridlike structure with pyrazolate bridges. As shown in Figure 3a, there are two approximately planar $[Cu(\mu\text{-}\mathbf{L}^1)]_2$ units, related by an inversion center, in which each $\mathbf{L}^1$ acts as a terdentate chelating−bridging linkage. In the binuclear unit, the distance of two Cu^{II} centers is 3.956 Å, being a little longer than those of **1** and **2**. The two binuclear units stack parallel and face-to-face (interplanar separation of 3.176−3.495 Å), with additional deprotonated ligands $\mathbf{L}^1$ perpendicular to the two $[Cu(\mu\text{-}\mathbf{L}^1)]_2$ planes forming linking "cross-pieces" between the $[Cu(\mu\text{-}\mathbf{L}^1)]_2$ units, and the adjacent nonbonding Cu···Cu distance between the units is 3.583 Å. In **3**, two of the metals (Cu2 and Cu2A) have additional nitrate anions attached and, therefore, have a N_4O environment which is the intermediate coordination geometry between square-pyramid and trigonal bipyramid, while Cu1 and Cu1A have square-pyramidal N_5 environments in which the pyridine donor atom is in the axial position and the axial ligand is significantly far from the metal [Cu1−N4 = 2.448(2) Å] than the four equatorial ligands (Cu−N lengths 1.970(2)−2.063(2) Å; see Table 4). The Cu1 center deviates from the mean equatorial plane defined by four coordinated nitrogen atoms toward the apical nitrogen atom by 0.114 Å, and the bond angles around that range from 74.07(8) to

Table 5. Selected Bond Distances (Å) and Angles (deg) for Complex **4**^{a}

Cu(1)−N(5)	1.952(4)	Cu(1)−N(2)	1.959(4)
Cu(1)−N(9)	1.991(4)	Cu(1)−N(1)	2.088(4)
Cu(1)−N(4)	2.356(4)	Cu(2)−N(3)	1.984(4)
Cu(2)−N(11)	2.013(4)	Cu(2)−N(8)	2.013(4)
Cu(2)−N(7)	2.084(4)	Cu(2)−N(6)$^{\#1}$	2.363(4)
Cu(2)−N(10)	2.477(4)		
N(5)−Cu(1)−N(2)	170.77(2)	N(5)−Cu(1)−N(9)	90.71(2)
N(2)−Cu(1)−N(9)	98.29(2)	N(5)−Cu(1)−N(1)	91.10(2)
N(2)−Cu(1)−N(1)	79.69(2)	N(9)−Cu(1)−N(1)	171.14(2)
N(5)−Cu(1)−N(4)	76.30(2)	N(2)−Cu(1)−N(4)	104.41(2)
N(9)−Cu(1)−N(4)	97.16(1)	N(1)−Cu(1)−N(4)	91.69(2)
N(3)−Cu(2)−N(11)	94.20(2)	N(3)−Cu(2)−N(8)	96.33(2)
N(11)−Cu(2)−N(8)	157.35(2)	N(3)−Cu(2)−N(7)	175.34(2)
N(11)−Cu(2)−N(7)	89.55(2)	N(8)−Cu(2)−N(7)	79.20(2)
N(3)−Cu(2)−N(6)$^{\#1}$	95.45(1)	N(11)−Cu(2)−N(6)$^{\#1}$	98.57(2)
N(8)−Cu(2)−N(6)$^{\#1}$	100.31(1)	N(7)−Cu(2)−N(6)$^{\#1}$	86.70(1)
N(3)−Cu(2)−N(10)	94.99(2)	N(11)−Cu(2)−N(10)	74.12(2)
N(8)−Cu(2)−N(10)	85.02(2)	N(7)−Cu(2)−N(10)	83.37(2)
N(6)$^{\#1}$−Cu(2)−N(10)	167.67(1)		

^{a} Symmetry codes: (#1) $-x + 1$, $-y + 2$, $-z$.

Table 6. Selected Bond Distances (Å) and Angles (deg) for Complex **5**^{a}

Cu(1)−N(2)	1.967(3)	Cu(1)−N(9)	1.977(3)
Cu(1)−N(5)	1.986(3)	Cu(1)−N(1)	2.064(3)
Cu(1)−N(4)	2.325(3)	Cu(2)−N(3)	1.961(4)
Cu(2)−O(1)	2.004(3)	Cu(2)−N(8)	2.023(3)
Cu(2)−N(7)	2.026(4)	Cu(2)−N(6)$^{\#1}$	2.085(3)
N(2)−Cu(1)−N(9)	97.54(1)	N(2)−Cu(1)−N(5)	165.64(1)
N(9)−Cu(1)−N(5)	92.39(1)	N(2)−Cu(1)−N(1)	80.03(1)
N(9)−Cu(1)−N(1)	176.89(1)	N(5)−Cu(1)−N(1)	89.65(1)
N(2)−Cu(1)−N(4)	113.96(1)	N(9)−Cu(1)−N(4)	93.69(1)
N(5)−Cu(1)−N(4)	75.50(1)	N(1)−Cu(1)−N(4)	89.09(1)
N(3)−Cu(2)−O(1)	94.14(2)	N(3)−Cu(2)−N(8)	95.58(1)
O(1)−Cu(2)−N(8)	116.43(2)	N(3)−Cu(2)−N(7)	175.33(2)
O(1)−Cu(2)−N(7)	87.08(2)	N(8)−Cu(2)−N(7)	79.85(2)
N(3)−Cu(2)−N(6)$^{\#1}$	91.60(2)	O(1)−Cu(2)−N(6)$^{\#1}$	119.76(2)
N(8)−Cu(2)−N(6)$^{\#1}$	122.53(1)	N(7)−Cu(2)−N(6)$^{\#1}$	91.70(2)

^{a} Symmetry code: (#1) $-x + 1/2$, $-y + 1/2$, $-z + 1$.

175.29(8)° (Table 4). It is noteworthy that the Cu2 ion is pentacoordinated to four nitrogen atoms of three distinct **L**^{1} ligands (Cu−N lengths 1.949(2)−2.062(2) Å) and one oxygen atom from the disordered nitrate anion (Cu−O = 2.188(1) Å). The bond angles around Cu2 range from 80.84(9) to 173.19(9)°, which is different from Cu1 in the coordination geometry. In addition, the ligand interplanar distances between two neighboring parallel [Cu(μ-**L**^{1})]$_2$ units of the adjacent tetranuclear molecules are ca. 3.4 Å, indicating the presence of face-to-face $\pi-\pi$ interactions that further stabilize the crystal structure and extend the tetranuclear molecule to a 1-D supramolecular chain.

[Cu$_4$(μ-L^1)$_6$L$^1_2$] (4). **4** is also a tetranuclear gridlike complex with pyrazolate bridges (Figure 3b), which is similar to **3** in the structure. Within this tetranuclear unit, the Cu···Cu distances is 3.977 (Cu1···Cu2) and 4.012 (Cu1···Cu2A) Å, respectively, and the interplanar separation of two approximately planar [Cu(μ-**L**^{1})]$_2$ units is 3.094−3.426 Å. However, it should be noted that the two metals (Cu2 and Cu2A) have an additional **L**^{1} attached and, therefore, have a N$_6$ environment, with a slight distorted octahedral coordination geometry [Cu−N bond lengths ranging from 1.984(4) to 2.477(4) Å] (Table 5). This feature is new in comparison with complex **3**.

The gridlike tetranuclear structure of **3** and **4** is similar to the analogous complexes [Cu$_4$(**L**^{1})$_6$(DMF)$_2$][PF$_6$]$_2$ (**8**)[2b,13] and [Cu$_4$(**L**^{1})$_6$(MeOH)$_2$][PF$_6$]$_2$ (**9**).[2b] Although all these compounds possess similar gridlike tetranuclear structure, there are many differences among them. First, in complexes **3**, **8**, and **9**, the coordination numbers of Cu^{II} ions are all 5, while these are 5 and 6 in complex **4**, and the coordination geometries of metal centers are quite different: square-pyramid and the intermediate coordination geometry between square-pyramid and trigonal bipyramid in **3**, square-pyramid and octahedron in **4**, and only square-pyramid in **8** and **9**, respectively. Second, in all the metal centers of square-pyramidal coordination geometry, the atoms in the axial position are different (pyridine N donor in **3** and **4**, one of the pyrazole N donor or oxygen atom of coordinated solvent molecule in **8** and **9**) (Figure S1). Third, in **8** and **9** there are two coordinated neutral solvent molecules, so the gridlike tetranuclear structure itself is not neutral and there are counteranions in the crystal structure; thus, the packing patterns are very different from those of complexes **3** and **4**.

[Cu$_4$(μ-L^1)$_6$(μ-L^2)]$_n$ (5) and [Cu$_4$(μ-L^1)$_6$(μ-L^3)]$_n$ (6). The structures of complexes **5** and **6** are similar and are both neutral 1-D chains constructed by the dicarboxylate ligands linking tetranucler Cu$_4$(μ-**L**^{1})$_6$ units which have structure similar to that in **3** (Figures 4 and 5). The only difference between **5** and **6** is the bridging dicarboxylate groups used. In **5**, 1,8-naphthalenedicarboxylate (**L**^{2}) attached to the two metal centers (Cu2 and Cu2A), while, in **6**, terephthalate (**L**^{3}) ligands bridge the adjacent tetranuclear units. In comparison with that of **3**, the coordination geometries of carboxylate-coordinated Cu^{II} ions are somewhat different in **5** and **6**, respectively. In **5**, there is a trigonal bipyramidal N$_4$O environment, in which the Cu2 (and Cu2A) center deviates from the equatorial plane defined by N8, N6A, and O1 (N8A, N6, and O1A) toward one of the apical nitrogen atoms (N3) by 0.133 Å, while, in **3**, there is an intermediate coordination geometry between square-pyramid and trigonal bipyramid. The geometry of all Cu^{II} centers in **6** is distorted square-pyramidal which is also different from that of **3**. Selected bond distances and angles are listed in Tables 6 and 7. The geometries of the Cu^{II} ion can be deduced in detail from these tables.

{[Cu$_4$(μ-L^1)$_4$(μ-L^4)$_2$](H$_2$O)$_3$}$_n$ (7). The structure of **7** consists of two kinds of 1-D neutral coordination chains (type **A** and type **B**), which are very similar except for slight differences in bond lengths and bond angles. The selected bond distances and angles are listed in Table 8. Herein type **A** is described in detail. As shown in Figure 6a, there are two independent Cu^{II} ions (Cu1 and Cu2) in the crystallographic asymmetric unit, which adopt different coordination geometries. The Cu1 is pentacoordinated to three nitrogen atoms of two distinct **L**^{1} ligands (Cu−N lengths 1.954(5)−2.041(5) Å) and two oxygen atoms from two distinct **L**^{4} ligands (Cu−O lengths 1.981(4)−2.294(5) Å) to form a distorted square-pyramid geometry. The Cu^{II} center deviates from the mean equatorial plane defined by three coordinated nitrogen atoms and one oxygen atom (O2) from

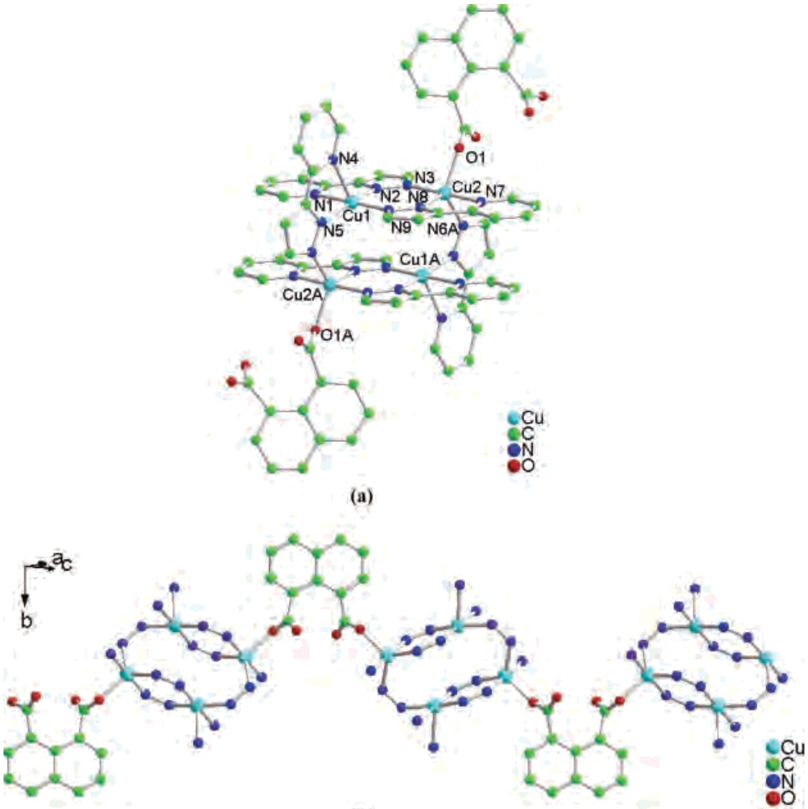

(a)

(b)

Figure 4. (a) View of the coordination environments of ligands and Cu^{II} ions in **5**. (b) 1-D chain structure of **5** (all carbon atoms on **L**^{1} ligands omitted for clarity).

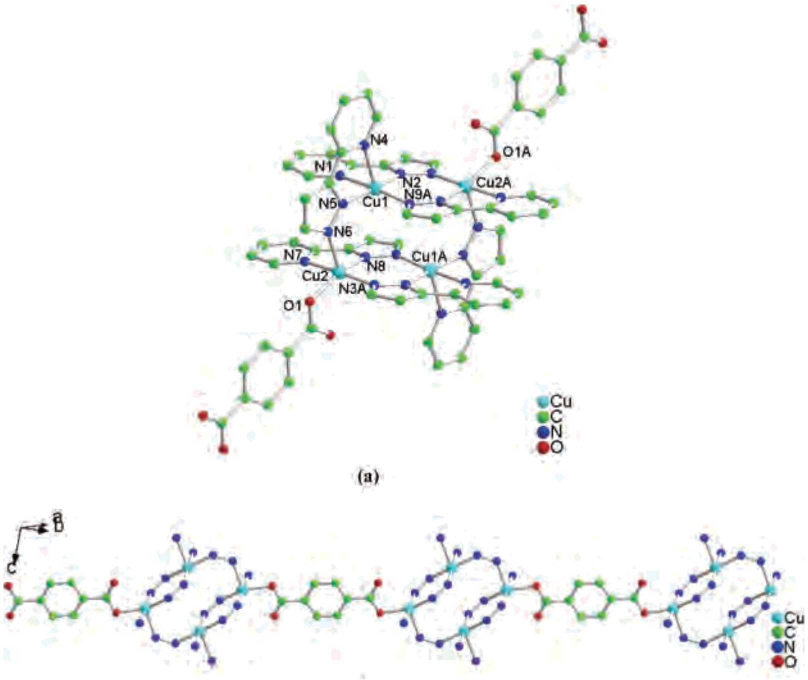

(a)

(b)

Figure 5. (a) View of the coordination environments of ligands and Cu^{II} ions in **6**. (b) 1-D chain structure of **6** (all carbon atoms on **L**^{1} ligands omitted for clarity).

one **L**^{4} ligand toward the apical O1, which is separated from another **L**^{4} ligand by 0.954 Å, and the bond angles around the Cu^{II} center range from 80.9(2) to 177.8(2)°. However, Cu2 adopts a distorted octahedral geometry coordinated by three nitrogen atoms from two distinct **L**^{1} ligands, one nitrogen atom and two oxygen atoms of one **L**^{4} ligand (Cu−N lengths 1.971(5)−2.093(6) Å and Cu−O lengths 2.282(5)−2.490 Å), and the bond angles around the Cu^{II} center range from 74.07(8) to 175.29(8)°. It is noteworthy that the Cu2−O2 distance is 2.490 Å, which is longer than

Table 7. Selected Bond Distances (Å) and Angles (deg) for Complex **6**^{a}

Cu(1)−N(2)	1.967(4)	Cu(1)−N(5)	1.971(4)
Cu(1)−N(9)$^{\#1}$	1.977(4)	Cu(1)−N(1)	2.078(4)
Cu(1)−N(4)	2.304(4)	Cu(2)−N(3)$^{\#1}$	1.959(4)
Cu(2)−N(8)	1.982(4)	Cu(2)−O(1)	2.020(3)
Cu(2)−N(7)	2.040(4)	Cu(2)−N(6)	2.212(4)
N(2)−Cu(1)−N(5)	167.84(2)	N(2)−Cu(1)−N(9)$^{\#1}$	97.82(2)
N(5)−Cu(1)−N(9)$^{\#1}$	92.95(2)	N(2)−Cu(1)−N(1)	79.54(2)
N(5)−Cu(1)−N(1)	89.13(2)	N(9)$^{\#1}$−Cu(1)−N(1)	173.31(2)
N(2)−Cu(1)−N(4)	107.58(2)	N(5)−Cu(1)−N(4)	76.77(2)
N(9)$^{\#1}$−Cu(1)−N(4)	95.74(2)	N(1)−Cu(1)−N(4)	90.92(2)
N(3)$^{\#1}$−Cu(2)−N(8)	96.93(2)	N(3)$^{\#1}$−Cu(2)−O(1)	91.71(2)
N(8)−Cu(2)−O(1)	156.01(2)	N(3)$^{\#1}$−Cu(2)−N(7)	175.42(2)
N(8)−Cu(2)−N(7)	80.40(2)	O(1)−Cu(2)−N(7)	89.37(2)
N(3)$^{\#1}$−Cu(2)−N(6)	93.05(2)	N(8)−Cu(2)−N(6)	107.67(2)
O(1)−Cu(2)−N(6)	94.11(1)	N(7)−Cu(2)−N(6)	91.31(2)

^{a} Symmetry code: (#1) $-x + 1, -y, -z$.

Table 8. Selected Bond Distances (Å) and Angles (deg) for Complex **7**

Cu(1)−N(6)	1.954(5)	Cu(1)−N(2)	1.969(5)
Cu(1)−O(2)	1.981(4)	Cu(1)−N(1)	2.041(5)
Cu(1)−O(1)	2.294(5)	Cu(2)−N(5)	1.971(5)
Cu(2)−N(3)	1.975(5)	Cu(2)−N(7)	2.070(6)
Cu(2)−N(4)	2.093(6)	Cu(2)−O(3)	2.282(5)
Cu(2)−O(2)	2.490(5)	Cu(3)−N(13)	1.950(5)
Cu(3)−N(9)	1.973(5)	Cu(3)−O(7)	1.980(4)
Cu(3)−N(8)	2.029(5)	Cu(3)−O(8)	2.315(5)
Cu(4)−N(12)	1.976(6)	Cu(4)−N(10)	1.982(5)
Cu(4)−N(14)	2.048(6)	Cu(4)−N(11)	2.077(5)
Cu(4)−O(5)	2.319(5)	Cu(4)−O(7)	2.379(4)
N(6)−Cu(1)−N(2)	96.9(2)	N(6)−Cu(1)−O(2)	93.7(2)
N(2)−Cu(1)−O(2)	153.8(2)	N(6)−Cu(1)−N(1)	177.8(2)
N(2)−Cu(1)−N(1)	80.9(2)	O(2)−Cu(1)−N(1)	88.1(2)
N(6)−Cu(1)−O(1)	90.2(2)	N(2)−Cu(1)−O(1)	101.6(2)
O(2)−Cu(1)−O(1)	102.2(2)	N(1)−Cu(1)−O(1)	90.5(2)
N(5)−Cu(2)−N(3)	96.3(2)	N(5)−Cu(2)−N(7)	162.8(2)
N(3)−Cu(2)−N(7)	93.4(2)	N(5)−Cu(2)−N(4)	80.4(2)
N(3)−Cu(2)−N(4)	175.7(2)	N(7)−Cu(2)−N(4)	90.5(2)
N(5)−Cu(2)−O(3)	118.3(2)	N(3)−Cu(2)−O(3)	91.0(2)
N(7)−Cu(2)−O(3)	75.6(2)	N(4)−Cu(2)−O(3)	88.3(2)
N(3)−Cu(2)−O(2)	90.6(3)	N(4)−Cu(2)−O(2)	92.2(5)
N(5)−Cu(2)−O(2)	93.9(2)	N(7)−Cu(2)−O(2)	71.7(6)
O(3)−Cu(2)−O(2)	147.4	N(13)−Cu(3)−O(7)	90.9(2)
N(9)−Cu(3)−O(7)	154.7(2)	N(13)−Cu(3)−N(8)	178.9(2)
N(9)−Cu(3)−N(8)	81.3(2)	O(7)−Cu(3)−N(8)	90.1(2)
N(13)−Cu(3)−O(8)	93.8(2)	N(9)−Cu(3)−O(8)	89.9(2)
O(7)−Cu(3)−O(8)	113.3(2)	N(8)−Cu(3)−O(8)	85.4(2)
N(13)−Cu(3)−N(9)	97.9(2)	N(12)−Cu(4)−N(10)	97.2(2)
N(12)−Cu(4)−N(14)	165.1(2)	N(10)−Cu(4)−N(14)	91.8(2)
N(12)−Cu(4)−N(11)	80.5(2)	N(10)−Cu(4)−N(11)	176.1(2)
N(14)−Cu(4)−N(11)	91.2(2)	N(12)−Cu(4)−O(5)	116.4(2)
N(10)−Cu(4)−O(5)	91.2(2)	N(14)−Cu(4)−O(5)	75.1(2)
N(11)−Cu(4)−O(5)	87.0(2)	N(12)−Cu(4)−O(7)	94.3(2)
N(10)−Cu(4)−O(7)	91.6(2)	N(14)−Cu(4)−O(7)	73.5(2)
N(11)−Cu(4)−O(7)	91.7(2)	O(5)−Cu(4)−O(7)	148.5(2)

other Cu−O lengths in this complex, indicating weak coordination.

Similar to **1**−**6**, in **7** two $\mathbf{L}^1$ ligands bridge two Cu^{II} centers to form an approximately planar [Cu(μ-$\mathbf{L}^1$)]$_2$ binuclear unit, and the two planar [Cu(μ-$\mathbf{L}^1$)]$_2$ units which stack parallel and face-to-face (interplanar separation 3.347−3.661 Å) are linked to a tetranuclear gridlike Cu^{II} structure by two $\mathbf{L}^4$ ligands. Then these tetranuclear units are further bridged by O1 of $\mathbf{L}^4$ to form a 1-D chain along the *a* direction as shown in Figure 6b.

In the crystal, lattice water molecules are located between neutral chains of **A** and **B**. There exist strong intermolecular hydrogen bonds between the water molecules and O atoms (O4, O5, and O6) of $\mathbf{L}^4$. The D···A lengths are ranging from 2.840 to 2.996 Å. These strong hydrogen-bonding interactions lead to the formation of two-dimensional planar motif as shown in Figure 6c. In addition, the interplanar distance between two neighboring parallel pyridyl rings of the adjacent **A** chains is ca. 3.5 Å, and the corresponding centroid-to-centroid distance is ca. 3.6 Å, indicating the presence of strong face-to-face $\pi-\pi$ stackings that further stabilize the crystal structure.[18] These $\pi-\pi$ interactions extend the 2-D hydrogen-bonded plane to a 3-D framework (Figure 6c).

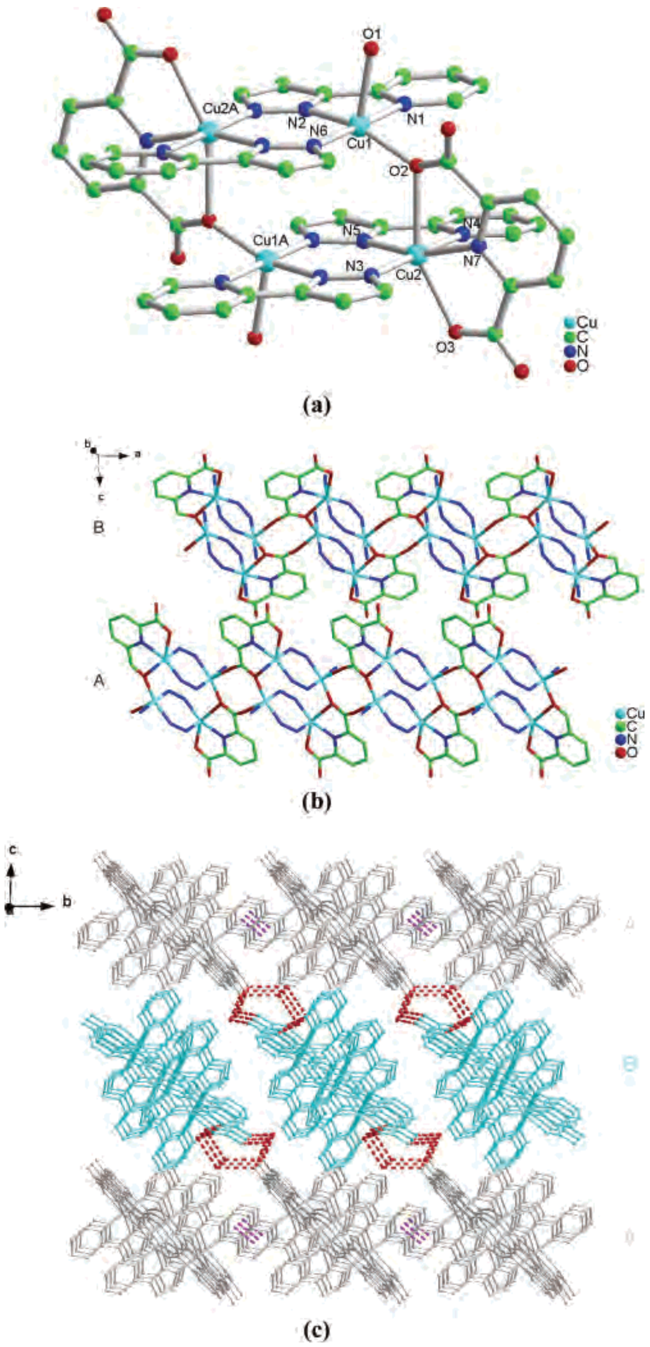

Figure 6. (a) View of the coordination environments of ligands and Cu^{II} ions in **7**. (b) Two types of 1-D chain structures in **7** (the lattice water molecules and all carbon atoms on $\mathbf{L}^1$ ligands omitted for clarity). (c) 3-D network structure of **7** formed through H-bonding and $\pi-\pi$ interactions.

Table 9. Main Structural and Magnetic Parameters

	dinuclear		tetranuclear (S−S)[a]		tetranuclear (S−L)[b]		
param	**1**	**2**	**3**	**5**	**4**	**6**	**7**
d(Cu−Cu) (Å)	3.920	3.920	3.956	3.988	3.977	3.951	3.961(3.936)
			3.583	3.578	4.012	3.906	3.727 (3.676) (oxo bridge)
d(Cu−N) (Å)	1.959[c]	1.967[c]	1.970[c]	1.981[c]	1.988[c]	1.971[c]	1.967 (1.971)[c]
			2.018[c]	2.036[c]	1.952	1.971	1.981 (1.981)
					2.363	2.212	2.490 (2.379) (oxo bridge)
torsion four N (deg)	0	0	1.6	0.4	1.7	3.9	2.6 (2.4)
Cu−N−N−Cu dihedral (deg)	3.3	18.3	5.9	0.9	5.6	4.0	7.0 (10.6)
			11.1	3.2	0.2	5.9	0.6 (3.0)
			8.7	0.6	3.2	5.1	
τ	0.29	0.03	0.12	0.93	0.30	0.10	0.22 (0.18)
			0.41	0.19	0.007	0.32	0.40 (0.40)
J (cm^{-1})	−211	−210	−126	−57.0	−173	−181	−184
			−47.5	−33.1			
ρ (%)	0.5	0.8	1.8	1.3	1.3	1.6	0.4

[a] Short−short Cu−N distances between the two binuclear entities. [b] Short−long Cu−N distances between the two binuclear entities. [c] The average value.

General Considerations on Magnetic Properties of Complexes 1−7. Complexes **1**−**7** have the same planar $[Cu(\mu\text{-}\mathbf{L}^1)]_2$ binuclear entities in which each Cu^{II} is linked by the $\mathbf{L}^1$ ligands. From the magnetic point of view, all complexes with this kind of bridging ligand show strong antiferromagnetic coupling.[6a] Indeed, theoretical considerations have been developed to understand this behavior: MO calculations indicate that the antiferromagnetic coupling is always very strong.[6c] A J value of -536 cm^{-1} has been reported for one of these Cu^{II} double diazine complexes.[6d] We reported very recently a complex with similar bridge, in which the J value was -368 cm^{-1}.[6a] The main factors that modify the $|J|$ parameter are the number of bridging ligands (double bridge better than only one bridge),[6a,b] the ring size (six-membered better than five-membered ring) and the diazine substituents. For a given diazine the geometry of the $Cu(N_2)_2Cu$ entity is very important. If the $(N_2)_2$ moiety is planar, without torsion, the $-J$ value increases; if the dihedral Cu−N−N−Cu angle is 0°, the maximum value of $-J$ can be expected. Finally, the Addison parameter τ[19] is crucial in the magnitude of $-J$. If τ is 0 (perfect square planar geometry), the overlap between the $d_{x^2-y^2}$ magnetic orbitals is active and perfect. This overlap diminishes when the tendency of the Cu^{II} geometry is toward $\tau = 1$ (trigonal bipyramidal geometry).

Magnetic Results. As predicted, the antiferromagnetic coupling for complexes **1**−**7** is very strong (see below). In these cases it is better to fit the χ_m data than the corresponding $\chi_m T$ ones, because when J is strongly antiferromagnetic the possible paramagnetic impurities that follow the Curie law are clearly visible in χ_m curves but not in $\chi_m T$ curves. For this reason, all J values gathered in Table 9 are values calculated from χ_m data. The $\chi_m T$ data are given for all complexes as Supporting Information. The respective fits were always slightly different than those obtained from χ_m curves.

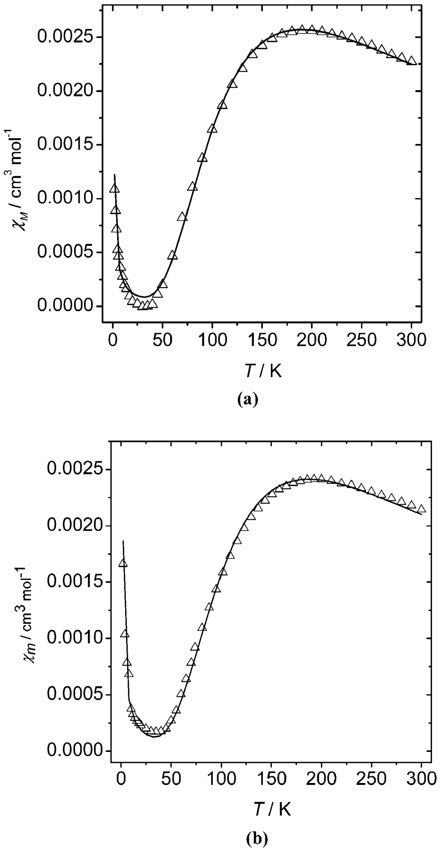

(a)

(b)

Figure 7. Plots of the susceptibility data, χ_M vs T, for (a) **1** and (b) **2**. Solid lines represent the best fit.

Furthermore, as indicated in other systems with strong antiferromagnetic coupling, when the diamagnetic correction is of the same order of magnitude as that of the uncorrected molar susceptibility, the uncertainty of the corrected values of χ_M is large, affording estimated J values reliable only within 5−10%.[20] This important fact originates another more difficult problem: the treatment of the TIP in this kind of complex. Currently the magnitude of the TIP parameter is of the same order of the diamagnetic correction (but with different sign) and is parametrized. Thus, if one is trying to draw some magneto−structural correlations, small variations in the TIP can obscure the results. For this reason, we have assumed an average TIP value for each Cu^{II} ion, exactly the

---

(19) Addison, A. W.; Rao, T. N.; Reedijk, J.; Rijn, J. V.; Verschoor, G. C. *J. Chem. Soc., Dalton Trans.* **1984**, 1349.

(20) Akhriff, Y.; Server-Carrió, J.; Sancho, A.; García-Lozano, J.; Escrivá, E.; Folgado, J. V.; Soto, L. *Inorg. Chem.* **1999**, *38*, 1174.

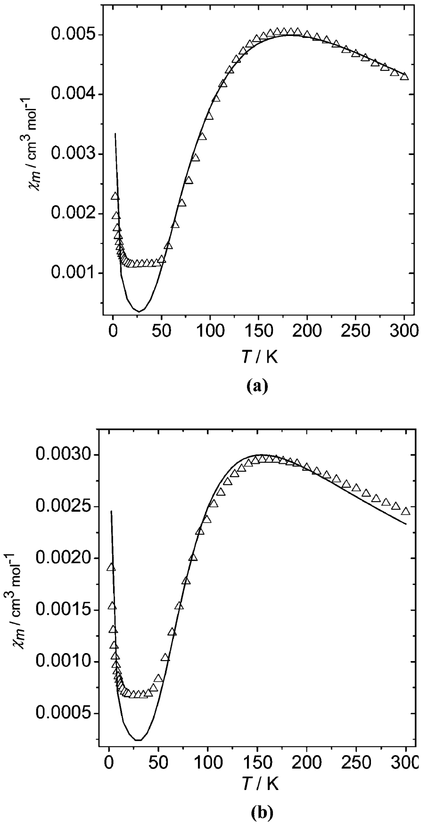

(a)

(b)

Figure 8. Plots of the susceptibility data, χ_M vs T, for (a) **3** and (b) **4**. Solid lines represent the best fit.

same for the seven complexes, of 75 × 10^{-6} cm^3 mol^{-1}, a little bit greater than that indicated in the literature[21] but much in accordance with our own experience in Cu^{II} complexes.

The magnetic properties of complexes **1**−**7** in the form of χ_M vs T plots (χ_m is the molar magnetic susceptibility for 2 or 4 Cu^{II} ions) are shown in Figures 7−9, respectively. The plots of χ_M show in all cases the typical signature for a strongly coupled binuclear Cu^{II} complex: there is a maximum close to 150−200 K which then decreases to, theoretically, 0 cm^3 mol^{-1}. However, at very low temperature there is an increasing, typical of these strongly coupled systems, that indicates the presence of small amount of paramagnetic impurities. The $\chi_M T$ curves (Figures S2−S4) are also indicative of this strong antiferromagnetic coupling: all curves start at ca. 0.7 cm^3 mol^{-1} K, lower than the value for two (or four) uncoupled unpaired electrons (0.375 × 2 or 4, assuming $g = 2.00$) and rapidly decrease to 0 at 2 K. As commented above, the presence of paramagnetic impurities is not evident in these curves.

The main structural parameters, J and ρ (impurities), are gathered in Table 9. To extract some magneto−structural correlations for these J values, we have divided the table in three parts, according to the nuclearity of the complexes. In the first part, we have indicated the complexes that are simply binuclear entities; the second part corresponds to tetranuclear complexes, in which two binuclear entities are linked by short−short N−Cu bonds. Finally, there are the complexes that are apparently tetranuclear but with their binuclear entities linked in Cu−N short−long manner. These complexes, although crystallographically can be seen as tetranuclear systems, from a magnetic point of view can be treated as binuclear entities. In some of these cases (see structural part) the tetranuclear units are linked by carboxylate bridges but at a very long distance. For this reason, considering the noticeable magnitude of J and for avoiding any overparametrization, these carboxylato bridges are omitted in the fitting procedure.

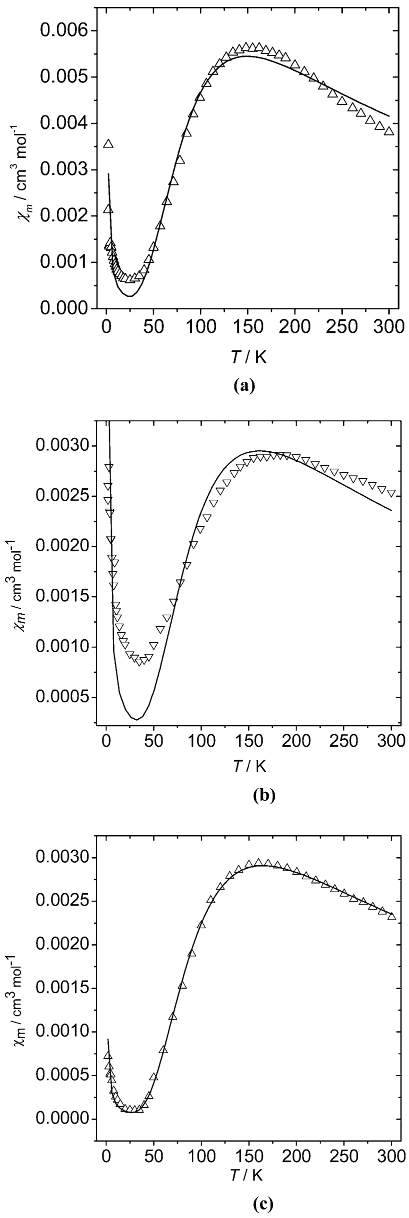

(a)

(b)

(c)

Figure 9. Plots of the susceptibility data, χ_M vs T, for (a) **5**, (b) **6**, and (c) **7**. Solid lines represent the best fit.

Dinuclear species (**1**, **2**) and pseudodinuclear species (**4**, **6**, and **7**) were fit by applying the known Bleaney−Bowers formula[22] for this kind of system, with the Hamiltonian $H = -J_i \sum S_i S_j$. Tetranuclear species were fitted through the formula given in the literature for a Cu$_4$ rectangle, with two

---

(21) Kahn, O. *Molecular Magnetism*; VCH Publishers: Weinheim, Germany, 1993. (Kahn gives as average value 60 × 10^{-6} cm^3 mol^{-1}.)

(22) Bleaney, B.; Bowers, K. D. *Proc. R. Soc. London, Ser. A* **1952**, *214*, 451.

kinds of J values, using the same Hamiltonian.[23] In all cases, the R factor, as the agreement factor defined as $\sum_i[(\chi_m T)_{obs} - (\chi_m T)_{calc}]^2/\sum_i[(\chi_m T)_{obs}]^2$, was very low, of the order of 10^{-5} or lower.

From Table 9 we can draw some interesting conclusions:

(a) The two "pure" dinuclear compounds have the same J value, close to -210 cm^{-1}. In both cases the torsion between the four nitrogen atoms is zero, but there is a significant difference in the Cu−N−N−Cu dihedral angle and τ parameter: in **1** the dihedral angle is small but τ is noticeable, whereas in **2** the dihedral angle is noticeable while τ is almost zero. This opposite difference can explain why the two J values are the same.

(b) The two tetranuclear complexes have one of the τ values close to 1 (**5**) indicating a quasi perfect tbp geometry. Complex **3** shows a τ parameter close to 0.5. This factor is the reason that can explain the smallest J value found in all this series of seven complexes. It must be stressed that when $\tau = 1$, the smallest J value can be expected. Indeed, in this case J is "only" -57 cm^{-1}. In the two compounds we can attribute the greatest J value to the double N−N bridge and the smallest to the single N−N bridge.

(c) Complexes **4**, **6**, and **7**, being structurally tetranuclear, can be treated as dinuclear ones from a magnetic point of view, due to the long−short distances between the binuclear entities. The three complexes show a J value close to -180 cm^{-1}. If we look at all parameters gathered in Table 9 for these three complexes, it can be deduced that the J value for **7** seems too strong, considering that one of the τ parameters is 0.4. But this complex is structurally different from the other six. First of all, there are two nonequivalent moieties in the crystal net, and mainly, the bridge between the two binuclear entities is a single oxo bridge. Even if the distances Cu−O are 1.9 and 2.4 Å, maybe the presence of a single-atom bridge obscures the true value for the Cu−NN−Cu bridges. All attempts to do the fit with two J values (as for **3** and **5**) failed, indicating a very strong correlation among them.

Finally, the X-band EPR spectra (Figure S5), recorded at room temperature, do not give any new information about the magnetic coupling of all these complexes. In some cases, when the antiferromagnetic character is very strong, the typical pattern for the $S = 1$ excited state can be seen, featuring the D parameter (zero-field splitting) of this state.[6a] However, in the seven complexes reported here, this feature has not been observed: the EPR spectra show only a broad band centered close to 3000 G (g close to 2.1). Only complex **2** shows a spectrum in which the D parameter seems to "appear" but is almost negligible.

Conclusion

Seven new Cu^{II} complexes containing a planar $[Cu(\mu\text{-}\mathbf{L}^1)]_2$ ($H\mathbf{L}^1$ = 3-(2-pyridyl)pyrazole) binuclear unit, generating from dinuclear (**1**, **2**) to tetranuclear (**3**, **4**) and then to 1-D (**5**, **6**, **7**) structures, have been prepared and structurally characterized. The structural comparison of **1**−**7** shows that assembly of these structures is directed by the stereochemical preference of the Cu^{II} ions: to fulfill this requirement necessitates deprotonation of the pyrazolyl groups to form the planar $[Cu(\mu\text{-}\mathbf{L}^1)]_2$ binuclear unit. The results of magnetic properties indicate all the complexes show very strong antiferromagnetic coupling (J are ranging from -33.1 to -211 cm^{-1}), and the main factors that affect the $|J|$ parameter are the geometries of the $Cu(N_2)_2Cu$ entity.

Acknowledgment. This work was financially supported by the National Science Funds for Distinguished Young Scholars of China (Grant 20225101), the National Natural Science Foundation of China (Grant 20373028), and the Spanish Government (Grant BQU2003-00539).

Supporting Information Available: X-ray crystallographic data for complexes **1**−**7** in CIF format, views of the coordination geometries of Cu^{II} ions in **3**, **4**, **8**, and **9** (Figure S1), plots of the susceptibility date (Figures S2−S4), and X-band EPR spectra (Figure S5) for **1**−**7**. This material is available free of charge via the Internet at http://pubs.acs.org.

IC051488D

---

[23] Jotham, R. W.; Kettle, S. F. A. *Inorg. Chim. Acta* **1970**, *4*, 145.